lysogenic strains contained retron Ec73 (Fig. 3C). Only one fragment was detected in lysogenized strains Cl-23, C367, and C368.

The 12.7-kb genome of retronphage ϕR73 can be shown as a circular map (Fig. 4) (*2*). The α gene is the only P4 gene that is essential for lytic growth (*3*), and retronphage ϕR73 can complement the α gene–defective P4 mutant. DNA synthesis of the retronphage ϕR73 genome could be primed by α primase at ORI and at two other sites, one at the 3′ end of *msd* and the other at the *attB* site. DNA synthesis initiating at *msd* would use msDNA as a primer and RT for DNA elongation. DNA synthesis initiating at *attB* would use selenocystyl tRNA as a primer and RT for DNA elongation. In both cases, RNA transcripts would be used as templates. The *E. coli* RT from retron Ec67 can use various primers and templates besides its own endogenous primer and template (*9*). It has not yet been determined whether such DNA synthesis participates in the life-cycle of retronphage ϕR73.

REFERENCES AND NOTES

1. M. Inouye and S. Inouye, *Trends Biochem. Sci.* **16**, 18 (1991).
2. J. Sun, M. Inouye, S. Inouye, *J. Bacteriol.*, in press.
3. L. E. Bertani and E. W. Six, in *The Bacteriophages*, R. Calendar, Ed. (Plenum, New York, 1988), vol. 2, p. 73.
4. Plasmid pCl-23a contains the 14.4-kb Bgl II–Eco RI fragment containing the entire ϕR73 that was cloned in pBR322 (*2*).
5. C366 is a P2*int*1 lysogen of Cl792 (*8*); the *int*1 mutation inactivates the P2 *int* gene and thereby blocks P2 prophage excision and coproduction of P2 after infection with P4-like phage.
6. E. W. Six, *Virology* **67**, 249 (1975).
7. We measured the latent period of ϕR73 infection by monitoring the optical density of the culture after infection. When infected cells lyse, the optical density drops, and the time required for the lysis is defined as the latent period.
8. W. Gibbs, R. Goldstein, R. Weiner, B. Lindquist, R. Calendar, *Virology* **53**, 24 (1973).
9. B. C. Lampson, M. Viswanathan, M. Inouye, S. Inouye, *J. Biol. Chem.* **265**, 8490 (1990).
10. J. T. Walker and D. H. Walker, *J. Virol.* **45**, 1118 (1983).
11. M. C. Birnboim and J. Dolly, *Nucleic Acids Res.* **7**, 1513 (1979).

12. Electron microscopy services were provided by the University of Iowa Central Electron Microscopy Research Faculty. We thank D. Cue for his help with the electron microscopy. Supported by NIH grant GM44012 (M.I. and S.I.) and AI04043 (E.W.S.)

21 November 1990; accepted 21 February 1991

Spectral Tuning of Pigments Underlying Red-Green Color Vision

MAUREEN NEITZ, JAY NEITZ, GERALD H. JACOBS*

Variations in the absorption spectra of cone photopigments over the spectral range of about 530 to 562 nanometers are a principal cause of individual differences in human color vision and of differences in color vision within and across other primates. To study the molecular basis of these variations, nucleotide sequences were determined for eight primate photopigment genes. The spectral peaks of the pigments specified by these genes spanned the range from 530 to 562 nanometers. Comparisons of the deduced amino acid sequences of these eight pigments suggest that three amino acid substitutions produce the approximately 30-nanometer difference in spectral peaks of the pigments underlying human red-green color vision, and red shifts of specific magnitudes are produced by replacement of nonpolar with hydroxyl-bearing amino acids at each of the three critical positions.

HUMAN COLOR VISION ENCOMpasses a range of individual variations, including the classically defined categories of anomalous and defective color vision (*1*) and a range of more subtle variations among individuals whose color vision is considered to be normal (*2, 3*). One of the principal causes of these color vision differences is variation in the spectral positioning of the cone photopigments. In turn, the spectral tuning of visual pigments is thought to be governed by interactions between the 11-*cis* retinal chromophore and the apoprotein, opsin (*4–6*). An essential step toward understanding the molecular basis of color blindness and other color vision variations is, thus, to determine the structural variations among opsins that govern the spectral absorption properties of the visual pigments.

Department of Psychology and Neuroscience Research Institute, University of California, Santa Barbara, CA 93106.

*To whom correspondence should be addressed.

We have identified amino acid substitutions likely to be involved in tuning the absorption spectra of naturally occurring visual pigments that underlie red-green color vision by comparing the deduced amino acid sequences of eight cone pigments with absorption peaks between 530 and 562 nm. These pigments are a middle wavelength–sensitive (MWS) pigment from a human protanope (7), a long-wavelength–sensitive (LWS) pigment from a human deuteranope, and three pigments from each of two species of South American monkey [squirrel monkeys (*Saimiri sciureus*) and saddle-backed tamarins (*Saguinus fuscicollis*)]. The genes encoding all of these visual pigments reside on the X chromosome (*8– 10*). The monkeys have a single X-chromosome locus with three allelic genes.

Spectral sensitivities of the pigments (Fig. 1) were determined by analysis of a retinal gross potential, the electroretinogram (ERG), recorded from the eye of each subject. To measure relative sensitivity, we adjusted the quantal intensity of a rapidly flickering monochromatic light to produce a response that matched in amplitude the response to an interleaved flickering reference light. Repetition of this procedure for many test wavelengths yielded a curve that characterizes the absorption spectra in dichromatic subjects of cone pigments that are sensitive to middle to long wavelengths (*7, 8, 11*).

Of the six exons composing X-linked visual pigment genes, only exons 2 to 5 specify membrane-spanning regions of opsin (*10*), and thus only these exons are likely to be linked to spectral tuning of the photopigments. Gene segments corresponding to these exons were amplified in genomic DNA from each animal with the polymerase chain reaction (PCR), and the nucleotide sequences were determined (*12*). No polymorphisms were found in the pigment gene sequences from individual monkeys, confirming that each has a single X-encoded pigment (*8, 9*). This was also true of the human deuteranope. The deduced amino acid sequences of the monkey pigments are from 96% to >98% identical to the human LWS pigment.

Which amino acid substitutions might account for the spectral differences among these? The human protanope and deuteranope pigments differ by 11 amino acid substitutions; seven of these are nonhomologous substitutions (Fig. 2A). A subset of these seven most likely accounts for the approximately 30-nm difference in the absorption maxima of the photopigments. Three of the monkey pigments have spectral peaks (556, 547, and 541 nm) that are clearly intermediate to those of the human pigments. Three pairwise comparisons can be made among the monkey pigments in which each pair differs at only one of the seven positions where nonhomologous substitutions occur between the human pigments. The 556-nm tamarin pigment differs

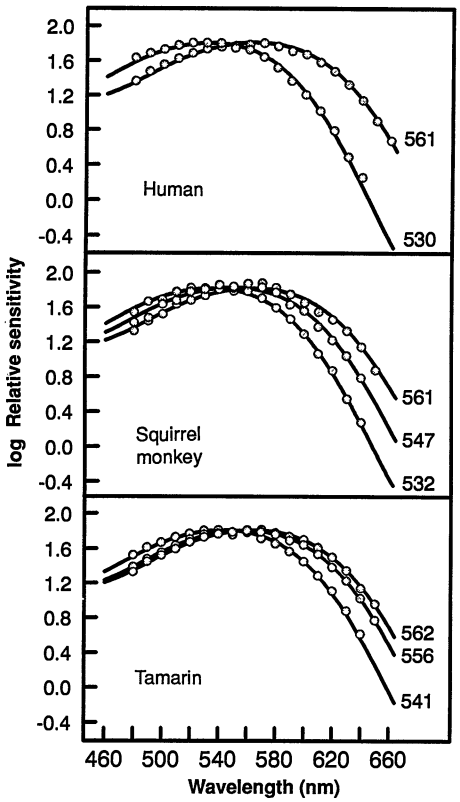

Fig. 1. Spectral sensitivities of eight cone pigments sensitive to middle to long wavelengths. The numbers to the right of the pigments are the absorption maxima of the pigments in nanometers. Pigments with five significantly different spectral positions are represented in these eight subjects. ERG sensitivity values are corrected for preretinal absorption by the lenses of the different species (*8, 9, 16*). The wavelength of peak sensitivity for each was determined by translation of a standard visual pigment absorption curve (*17*) on a log-wavenumber axis to obtain the best fit. The curve with the best fit for each is indicated by the solid line.

from the 547-nm squirrel monkey pigment at position 277; the tamarin 556-nm and 562-nm pigments differ at position 180, and the tamarin 556-nm and 541-nm pigments differ at position 285. The cumulated shift in spectra between these three pairs of monkey pigments is approximately 30 nm (Fig. 2A). This suggests that these replacements of nonpolar residues with hydroxyl-bearing amino acids at positions 180, 277, and 285 may account for the 30-nm red shift between the human pigments.

If these three are the only substitutions that produce spectral shifts among the eight pigments studied here, and if their effects are simply cumulative, then the separation in spectral peaks between any pair of pigments should be predicted by the amino acid differences between them at the three positions. For example, pigments that are identical at positions 180, 277, and 285 should have identical spectra, pigments that differ at all three positions should differ by approximately 30 nm, and pairs of pigments that differ by a subset of the three should have intermediate spectral separations. The observed spectral differences between pigment pairs compared to those predicted by the hypothesis that additive effects of changes at amino acid positions 180, 277, and 285 account for all shifts in spectra among these pigments are shown in Fig. 2B. The best fit between observed and predicted spectral differences is obtained if the shifts produced by the individual substitutions are as follows: position 180, 5.33 nm; position 277, 9.5 nm; and position 285, 15.5 nm. The correspondence between predicted and observed values is good; the observed shifts never differed from those predicted by the hypothesis by more than 2 nm, a value within the error of our spectral measurements.

If the spectral differences between the monkey pigments are produced by the same set of substitutions that regulate the difference between the two human pigments, then the only solution to the problem of which changes govern the spectral difference between the human pigments is the one given above. However, there are two nonhomologous substitutions among the monkey pigments that do not occur between the human protanope and deuteranope pigments. If these are considered, are there alternatives to the solution given above?

Twenty amino acid positions vary among the eight visual pigments examined (Table 1). The substitutions at 11 of these positions are unlikely to be involved in spectral tuning because they involve amino acids with side groups having similar chemical characteristics (61, 111, 115, 116, 173, 174, 236, 274, 275, 279, and 320) or they occur in loops of the pigment (115, 115, and 298) that are not believed to be embedded in the membrane (*10, 13*). Hydroxyl-bearing amino acids are substituted for nonpolar residues at the remaining eight positions, which include six amino acids that distinguish human MWS and LWS pigments (Table 1, A through G). These could alter the charge distribution in the chromophore microenvironment and thus may regulate the absorption spectra. The substitutions at positions 230 and 233 are grouped because substitutions at these positions never occurred independently in the pigments we studied.

The most informative comparisons of amino acid differences with spectral differences are summarized in the form of the equations in which the sum of the candidate substitutions that occur between two pigments is set equal to the magnitude of the red shift between them (Table 2). Substitution of hydroxyl-bearing for nonpolar amino acids that are associated with red shifts were arbitrarily assigned positive values; substitutions of nonpolar for hydroxyl-bearing amino acids were assigned negative values. In Eqs. 1 to 3, three pairs of pigments differ by a single candidate substitution

A

Subject	Spectral peak	Amino acid number						
Humans		180	230	233	277	285	298	309
Deuteranope	561 nm	Ser	Ile	Ala	Tyr	Thr	Ala	Tyr
Protanope	530 nm	Ala	Thr	Ser	Phe	Ala	Pro	Phe
	diff = 31 nm							
Monkeys								
Tamarin	562 nm	**Ser**	Ile	Ala	Tyr	Thr	Ala	Tyr
Tamarin	556 nm	**Ala**	Ile	Ala	Tyr	Thr	Ala	Tyr
	diff = 6 nm							
Tamarin	556 nm	Ala	Ile	Ala	Tyr	**Thr**	Ala	Tyr
Tamarin	541 nm	Ala	Ile	Ala	Tyr	**Ala**	Ala	Tyr
	diff = 15 nm							
Tamarin	556 nm	Ala	Ile	Ala	**Tyr**	Thr	Ala	Tyr
Squirrel Monkey	547 nm	Ala	Ile	Ala	**Phe**	Thr	Ala	Tyr
	diff = 9 nm							

30 nm = Total shift produced by sum of changes at (180)+(277)+(285)

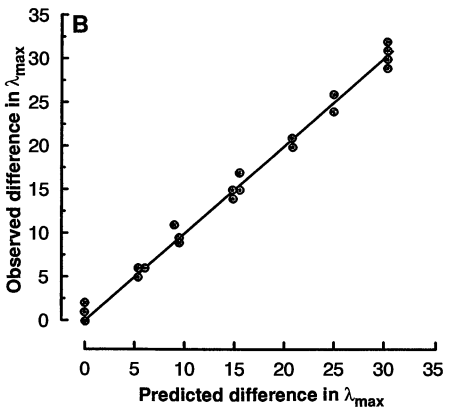

Fig. 2. (**A**) Seven nonhomologous amino acid substitutions distinguish human protanope and deuteranope pigments. Each of three pairs of monkey pigments differ at only one of the seven positions that distinguish the human pigments. The numbering system is from (*10*). (**B**) Twenty-eight paired comparisons among the eight visual pigments. Observed differences in spectral peak are plotted as a function of the differences in spectral peaks predicted by the hypothesis that only the substitutions at amino acid positions 180, 277, and 285 shift the absorption spectrum. The difference in spectrum between each pair of pigments was predicted from the amino acid differences between them at the three positions. Pigments that are identical at the three positions are predicted to have 0 difference in spectral peak. For pigments that differ at more than one of the three amino acid positions, the predicted difference in spectral peak is the sum of the spectral shifts produced by the individual substitutions. The magnitudes of the shifts produced by the three individual substitutions were varied so that the values that best fit could be determined. If the correspondence between observed and predicted values was perfect, all data points would lie on the line.

Table 1. Differences in deduced amino acid sequences of eight visual pigments sensitive to middle to long wavelengths. Results from partial sequences of cone pigments from rhesus monkey (*14*) are included for comparison. Boxes indicate residues identified in Fig. 2 as those involved in spectral tuning. Only residues that vary are shown. The labels above the numbered amino acid positions lettered A through G designate positions where substitutions occur that are candidates for producing spectral shifts (see text). (A, alanine; F, phenylalanine; I, isoleucine; L, leucine; M, methionine; P, proline; S, serine; T, threonine; V, valine; and Y, tryosine.)

Species	Spectral peak	Amino acid position																				
		A							B	C					D	E		F		G		
		61	65	111	115	116	173	174	180	230	233	236	274	275	276	277	279	285	298	309	320
*Rhesus monkey	LWS												I	F	A	Y	V	T	A	Y	I
Human deuteranope	561	I	T	I	V	S	I	A	S	I	A	M	I	F	A	Y	V	T	A	Y	V
Squirrel monkey	561	I	T	I	V	S	V	A	S	I	A	M	I	M	A	Y	V	T	A	Y	I
Tamarin	562	L	V	V	V	Y	V	A	S	I	A	M	I	V	A	Y	V	T	A	Y	I
Tamarin	556	L	V	V	V	Y	I	A	A	I	A	M	I	A	A	Y	V	T	A	Y	I
Squirrel monkey	547	I	T	V	V	Y	V	V	A	I	A	M	I	L	T	F	I	T	A	Y	I
Tamarin	541	L	V	V	I	Y	I	A	A	I	A	M	I	L	A	Y	V	A	A	Y	I
Squirrel monkey	532	I	T	I	V	S	V	A	A	T	S	V	I	V	T	F	I	A	A	Y	I
Human protanope	530	I	T	I	V	S	I	A	A	T	S	V	V	L	A	F	F	A	P	F	V
*Rhesus monkey	MWS												F	L	A	F	F	A	A	Y	I

each. The effects of these individual substitutions are unequivocal. (The measured 1-nm difference between the pigments in Eq. 1 is not significantly different from 0.) In Eq. 4, squirrel monkey 532 and 547 pigments differ only by substitutions C and F. The effect of F is determined in Eq. 3. The spectral difference between the two pigments of Eq. 4 is the same as that produced by F alone. The substitutions labeled C, thus, do not appear to influence the pigment spectra. In Eqs. 5 and 6, substitutions D, E, and G do not occur singly between any of the pigments studied. These equations can be simplified by assuming that over this limited spectral range, substitutions that influence the spectra have approximately additive effects.

From these comparisons, unique determinations can be made for the effects of four of the candidate substitutions (Table 1, A, B, C, and F). A red shift of 21 nm between human LWS and MWS pigments is accounted for by addition of the effects of changes at positions 180 and 285 (shifts of about 5.33 and 15.5 nm, respectively). How the remaining 9- to 10-nm difference between the human pigments is distributed between positions 277 and 309 (Table 2, Eq. 6) cannot be uniquely determined from these comparisons.

Table 2. Equations describing the relation of amino acid substitutions between pairs of pigments to the spectral differences between the pigments. The letters (A through G) refer to amino acid positions in Table 1. (Subscript t, tamarin; subscript h, human; and subscript s, squirrel monkey.)

Equations	Solutions
1. $562_t - 561_h = -A$	A = 0
2. $562_t - 556_t = B$	B = 6
3. $556_t - 541_s = F$	F = 15
4. $547_s - 532_s = F - C$	C = 0
5. $556_t - 547_h = -A + E - D$	E − D = 9
6. $561_h - 530_h = B + C + E + F + G$	E + G = 10

For two reasons, we argue that the solution suggested in Fig. 2A is the correct one; that is, the substitution at position 277 produces the remaining 9- to 10-nm difference. First, replacement of Ala^{285} with Thr^{285} produced a red shift, suggesting that the threonine hydroxyl group acts near the protonated Schiff base nitrogen (*6*). Residues 276 and 309 are positioned so any interaction would also be near the Schiff base end of the chromophore. Hydroxyl-bearing groups at these positions, if they interact with the chromophore, would also be expected to produce red shifts. This is contrary to the solutions of Table 2 (Eqs. 5 and 6), which require any significant effect of replacing Ala^{276} with Thr^{276} to produce a shift in the opposite direction to that of replacing Phe^{309} with Tyr^{309}. The only solution that does not require this opposing effect is that neither substitution produces a shift in the spectrum. Support for this argument is also found from examination of the partial sequences of the MWS and LWS pigments of the macaque monkey (*14*). The spectral separation between these pigments (*15*) is nearly identical to that between the human protanope and deuteranope pigments. These pigments differ at position 277, but do not differ at position 276 or 309 (Table 1).

These results suggest that the spectral differences among these middle to long-wavelength pigments are determined by the additive effects of substitutions at three amino acid positions. This has implications for the understanding of the molecular basis for human color-vision variations. Nathans and co-workers (*10*) characterized an LWS pigment gene isolated from genomic DNA of a male with normal color vision and two LWS pigment genes from a cDNA library representing several dozen human eyes. The LWS pigments encoded by the two cDNAs differ from that encoded by the genomic gene by a single nonconserved amino acid substitution—Ala^{180} for Ser^{180}. Our experiments show that these two LWS pigments differ in spectral peak by 5 to 6 nm. Given the incidence of color-defective vision, it is unlikely that both LWS pigment cDNAs could have been drawn from color blind eyes, and thus there may be two LWS pigments separated by 5 to 6 nm present in the population with normal color vision. A polymorphism in LWS cone pigments of this nature may explain variations in red-green color vision among people with normal color vision (*3*).

REFERENCES AND NOTES

1. J. Pokorny, V. C. Smith, G. Verriest, A. J. L. G. Pinckers, *Congenital and Acquired Color Vision Defects* (Grune & Stratton, New York, 1979).
2. J. Neitz and G. H. Jacobs, *Nature* **323**, 623 (1986).
3. _____, *Vision Res.* **30**, 621 (1990).
4. T. P. Sakmar, R. R. Franke, H. G. Khorana, *Proc. Natl. Acad. Sci. U.S.A.* **86**, 8309 (1989).
5. E. A. Zhukovsky and D. D. Oprian, *Science* **246**, 928 (1989).
6. E. M. Kosower, *Proc. Natl. Acad. Sci. U.S.A.* **85**, 1076 (1988).
7. J. Neitz, M. Neitz, G. H. Jacobs, *Nature* **342**, 679 (1989).
8. G. H. Jacobs and J. Neitz, *Proc. Natl. Acad. Sci. U.S.A.* **84**, 2545 (1987).
9. _____, M. Crognale, *Vision Res.* **27**, 2089 (1987).
10. J. Nathans, D. Thomas, D. S. Hogness, *Science* **232**, 193 (1986).
11. J. Neitz and G. H. Jacobs, *J. Opt. Soc. Am. A* **1**, 1175 (1984).
12. Duplicate samples of genomic DNA isolated from blood or tissue from individual subjects were used in the PCR. Reactions were carried out in a Perkin-Elmer Cetus thermal cycler for 35 cycles as follows: 94°C for 30 s, 55°C for 30 s, and 72°C for 30 s. The reactions were then incubated at 72°C for 10 min. Reagents were those provided with the Amplitaq kit (Perkin-Elmer Cetus). Each of exons 2, 3, 4, and 5 of the pigment genes sensitive to middle to long wavelengths were amplified separately. Primers were 18-base oligonucleotides corresponding in sequence to that encoding the first six amino acids and complementary to sequences encoding the last six amino acids specified by each exon. The pigment gene sequences from which primer sequences were derived are invariant across the six human MWS and LWS cone pigment genes in (*10*). Amplified DNA sequences were purified on a 5% polyacrylamide gel and ligated into the plasmid vector, Bluescript (Stratagene), and the nucleotide sequence of both strands of pigment-gene DNA segments was determined (*18*). For exons 3 and 5, aliquots of amplified DNA were also used in asymmetric PCR to generate single-stranded DNA (*19*) corresponding to each of the DNA strands, and the nucleotide sequence was determined.
13. E. A. Dratz and P. A. Hargrave, *Trends Biochem. Sci.* **8**, 128 (1983).
14. C. J. Green, personal communication.

15. B. J. Nunn, J. L. Schnapf, D. A. Baylor, *Nature* **309**, 264 (1984).
16. G. Wyszecki and W. S. Stiles, *Color Science* (Wiley, New York, 1982).
17. S. M. Dawis, *Vision Res.* **21**, 1427 (1981).
18. F. Sanger, S. Nicklen, A. R. Coulson, *Proc. Natl. Acad. Sci. U.S.A.* **74**, 5463 (1977).
19. U. Gyllensten, *PCR Technology* (Stockton, New York, 1989).
20. We thank J. Nathans for providing probes for the X-linked photopigment genes and C. J. Green for providing the macaque monkey cone pigment sequences. Supported by NIH grants EY-07200 and EY-02052 and by NSF grant BNS-8910062.

21 November 1990; accepted 11 March 1991

Technical Comments

Detecting Potassium on Mercury

A. L. Sprague *et al.* (*1*) attribute an enhanced emission in the potassium (K) D lines on 14 October 1987 in the equatorial region of Mercury to a diffusion source centered on Caloris Basin. We believe that Sprague *et al.* misinterpreted the data.

The single observation of enhanced emission of K in the equatorial bin was followed 50 minutes later by a second observation that showed no enhancement (Table 1). The equatorial column abundance derived from the second observation was smaller by a factor of 3.6 and was similar to abundances observed before and after the enhanced emission. The average column abundance from the two is 2.3×10^9 K atoms cm^{-2}. This is similar to normal K abundances (0.5 to 1.0×10^9 K atoms cm^{-2}). The ratio of equatorial to polar column abundance appears to decrease by a factor of 2.5 in 50 minutes. This suggests the presence of noise in the measurement of enhanced emission.

If the source of the volatiles was primarily in the Caloris Basin region, then an enhanced emission should be correlated with the position of Caloris Basin for the entire body of observations. The illumination and viewing geometry of the 14 October observations closely match the discovery observation of 16 November 1985 (*2*). We resampled our data to match the binning of the 14 October data. The average zenith column abundance along the slit for the discovery observation was within 30% of the second observation from 14 October (Table 1). However, when we compared the discovery observation with the first observation from 14 October, we found a difference of a factor of 5. Similarly, the equator to pole ratio from the discovery observation matched the second observation from 14 October, but was a factor of 3.5 smaller than the first observation. In short, the discovery observation did not confirm the high K abundance reported by Sprague *et al.* over Caloris.

The emission intensity for the north polar region should be larger than that for the south polar region if there is a Caloris Basin source. The center of Caloris Basin is near 30° north latitude and extends roughly from the equator to about 60° north latitude. Atmospheric turbulence, usually affecting spatial resolution by 2 to 3 arc seconds, can smear the light from a source at 30° well up to northern latitudes. Sprague *et al.* grouped their observations into three bins, with the equatorial bin spanning the mid-half of the disk. Even with this wide bin, one would expect an asymmetric distribution (with the northern bin significantly larger than the southern bin), but the data do not show this. The discovery observations also do not show any significant north-to-south asymmetry.

Sprague *et al.* note that the behavior of sodium (Na) and K are expected to be similar. Consequently, another place to search for evidence of a Caloris Basin source would be in the published Na data for Mercury. R. M. Killen *et al.* (*3*) and A. E. Potter and T. H. Morgan (*4*) cite several instances of Na observation on Mercury. In the observations of 16 November (*4*) and 3 December 1986 (*3*), Caloris Basin was in view. The subsolar column abundances on these dates were the lowest that we have recorded. The equator-to-pole ratios are all near unity for the observations of Na in the paper by Killen *et al.* (Table 2), for the discovery observation of K, and for the second K observation of Sprague *et al.* These data do not support the conclusion of Sprague *et al.* that there is a significant vapor source at Caloris Basin.

Sprague *et al.* also point out that some of the Na images reported by Potter and Morgan (*5*) showed enhancements that approximately matched the location of Caloris Basin or its antipode. This is only part of the story, because most of the images that showed strong local enhancements showed *two* regions of high Na concentration. These appeared on the same side of the planet, centered at about 60° north and 50° south latitude. A single diffusion source at Caloris Basin could not account for north-to-south pairs of Na images on the same side of the planet. One could evoke multiple, time-variable, geologic sources to explain the emission peaks, but such explanations would not be convincing.

Table 1. Potassium observations (uncorrected for atmospheric turbulence).

Reference	Date	Time	Longitude of sub-Earth point	Longitude of sub-solar point	Phase	Disk average column abundance ($\times 10^9$)	Equator to pole ratio of column abundance
(*2*)	16 Nov. 1985	21:48	279	174	109	0.72	1.2
(*1*)	14 Oct. 1987	21:32	269	161	107	3.60	4.2
(*1*)	14 Oct. 1987	22:22	269	161	107	1.00	1.7

Table 2. Sodium observations (corrected for atmospheric turbulence).

Reference	Date	Longitude of sub-Earth point	Longitude of sub-solar point	Phase	Disk average column abundance ($\times 10^{11}$)	Equator to pole ratio of column abundance
(*3*)	2 Apr. 1987	24.5	102.1	77.6	1.78	1.0
(*3*)	3 Apr. 1987	29.4	105.5	76.1	2.42	1.0
(*3*)	6 Apr. 1987	43.9	115.4	71.6	0.68	1.3
(*3*)	13 Feb. 1987	92.7	0.08	92.6	2.60	1.0
(*3*)	3 Dec. 1986	127.2	188.7	63.2	0.80	1.0